

Analyst

Accepted Manuscript



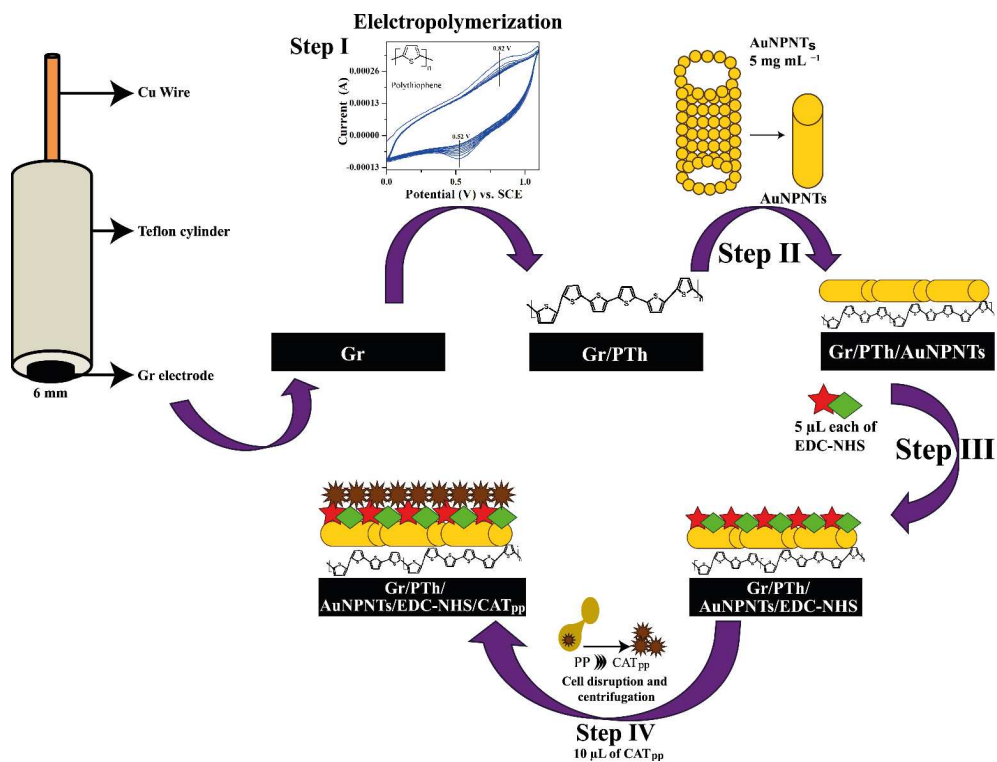
This is an *Accepted Manuscript*, which has been through the Royal Society of Chemistry peer review process and has been accepted for publication.

Accepted Manuscripts are published online shortly after acceptance, before technical editing, formatting and proof reading. Using this free service, authors can make their results available to the community, in citable form, before we publish the edited article. We will replace this *Accepted Manuscript* with the edited and formatted *Advance Article* as soon as it is available.

You can find more information about *Accepted Manuscripts* in the [Information for Authors](#).

Please note that technical editing may introduce minor changes to the text and/or graphics, which may alter content. The journal's standard [Terms & Conditions](#) and the [Ethical guidelines](#) still apply. In no event shall the Royal Society of Chemistry be held responsible for any errors or omissions in this *Accepted Manuscript* or any consequences arising from the use of any information it contains.

Table of contents entry



We present the development of electrochemical H_2O_2 biosensor using catalase derived from *Pichia pastoris* as a bioelectrocatalyst immobilized on gold nanoparticle-nanotubes and Polythiophene hybrid.

1
2
3 **Development of a simple bioelectrode for the electrochemical detection of hydrogen**
4 **peroxide using *Pichia pastoris* catalase immobilized on gold nanoparticle nanotubes and**
5 **polythiophene hybrid**
6
7
8
9

10
11 **Seetharamaiah Nandini,^a Seetharamaiah Nalini,^a Jakkid Sanetuntikul,^b Sangaraju**

12
13 **Shanmugam,^b Pathappa Niranjana,^{c,*} Jose Savio Melo^{d,*} and Gurukar Shivappa Suresh^{a,*}**

14
15
16 *^aDepartment of Chemistry and Research Centre, N.M.K.R.V. College for Women, Jayanagar,*
17
18 *Bangalore 560 011, India*

19
20
21 *^bDepartment of Energy Systems and Engineering, Daegu Gyeongbuk Institute of Science and*
22
23 *Technology, Daegu 711-873, Republic of Korea*

24
25
26 *^cDepartment of Biochemistry, Kuvempu University, Shankarghatta, Shimoga 577451, India*

27
28 *^dNuclear Agriculture and Biotechnology Division, Bhabha Atomic Research Centre, Mumbai*
29
30 *400 085, India*

31
32
33
34
35
36
37
38 **Corresponding authors*

39
40 *Telephone: 91-80-26654920*

41
42 *Fax no: 91-80-22453665*

43
44
45 *E-mail: sureshsmrv@yahoo.co.in (G.S. Suresh),*

46
47 *jsmelo@barc.gov.in (J.S. Melo) and*

48
49 *bpniru@gmail.com (P. Niranjana)*
50
51
52
53
54
55
56
57
58
59
60

Abstract

In this report a simple and innovative electrochemical H₂O₂ biosensor has been proposed using catalase (CAT) derived from *Pichia pastoris* as bioelectrocatalyst. The model biocomponent was immobilized on gold nanoparticle nanotubes (AuNPNTs) and polythiophene composite by means of 1-Ethyl-3-(3-dimethylaminopropyl)-carbodiimide and N-hydroxysuccinimide (EDC-NHS) coupling reagent. In this present work, we have successfully synthesized AuNPs by ultrasonic irradiation. The tubular gold nanostructures containing coalesced AuNPs were obtained by sacrificial template synthesis. The assembly of AuNPNTs onto the graphite electrode was achieved via S-Au chemisorptions. The latter was pre-coated with electropolymerized thiophene to enable S groups to bind AuNPNTs. The combination of AuNPNTs-PTh i.e., inorganic-organic hybrid provides a stable enzyme immobilization platform. The physical morphology of the fabricated biosensor Gr/PTh/AuNPNTs/EDC-NHS/CAT_{pp} was investigated using SEM and EDX. The analytical performance of the bioelectrode was examined using cyclic voltammetry, differential pulse voltammetry and chronoamperometry. Operational parameters such as working potential, pH and thermal stability of the modified electrode were examined. The beneficial analytical characteristics of the proposed electrode were demonstrated. Our results indicate that the Gr/PTh/AuNPNTs/EDC-NHS/CAT_{pp} bioelectrode exhibits wide linear range from 0.05 mM to 18.5 mM of H₂O₂, fast response time of 7 s, excellent sensitivity of 26.2 mA mM⁻¹ cm⁻², admirable detection limit of 0.12 μM and good Michaelis-Menten constant of 1.4 mM. Further the bioelectrode displayed good repeatability, high stability and acceptable reproducibility which can be attributed to the AuNPNTs-PTh composite that provides biocompatible micro-environment.

1. Introduction

Hydrogen peroxide (H_2O_2) is a well known oxidizing, bleaching and sterilizing agent. It is also one of the significant byproduct or substrate of many biological reactions.^{1,2} It plays an essential role in waste water treatment, paper, textile industry etc. Conversely, it is been recognized as chemical threat in the progression of many diseases like atherosclerosis, renal disease, ageing and others.³ As a result, there is a serious public concern for the selective, inexpensive and accurate determination of H_2O_2 . A variety of methodologies have been developed for the quantification of H_2O_2 , such as titrimetry, spectrometry, chemiluminescence and electrochemistry.⁴⁻⁶ However, due to the relative merits and demerits of these analytical techniques, electrochemical method is considered to be the most amenable and is receiving substantial interest owing to their convenience, efficiency, low cost, etc. A good number of electrochemical biosensors have been efficiently developed based on the electrocatalysis and direct electron transfer between the electrode and the immobilized enzyme or protein like horseradish peroxidase, hemoglobin etc.^{7,8} Nonetheless, the enzymatic electrochemical biosensors suffer from inherent annoyance like instability to the factors like pH, temperature, exposure to chemicals, elaborate immobilization procedure, high cost and easy distortion during fabrication, use and storage.⁹ Whilst, hemoglobin has been restricted, due to the lack of diverse electron transfer process owing to its large protein size and inaccessibility of the redox centre which is insulated from the conductive support by the peptide backbone.¹⁰ To circumvent these problems, it would be desirable and interesting to develop an electrochemical biosensor based on novel biological materials as bioelectrocatalyst that can transcend the limitations of enzymes/proteins.

1
2
3
4
5
6
7
8
9
10
11
12
13
14
15
16
17
18
19
20
21
22
23
24
25
26
27
28
29
30
31
32
33
34
35
36
37
38
39
40
41
42
43
44
45
46
47
48
49
50
51
52
53
54
55
56
57
58
59
60

Methylotrophic yeasts such as *Pichia pastoris* (*Pp*) are promising sources of redox enzymes in biotechnology.¹¹ They contain catalase (CAT) an important enzyme sequestered together with alcohol oxidase in peroxisomes.¹² However, *Pp* is always associated with about 200-400 fold higher catalase activity than that of alcohol oxidase. Studies have shown that CAT detected in *Pp* resembles the peroxisomal CAT A of *Saccharomyces cerevisiae*, which is well documented to contain mitochondrial CAT.¹³ Active peroxisomal CAT [E.C.1.11.1.6] of approximately 240 kD is a homotetramer made up of four polypeptide chain each over 500 amino acids long and it contains four porphyrin heme as co-factor that allows enzyme to decompose H₂O₂ into water and oxygen.¹⁴

In recent years, advances in bionanoelectrochemistry have been centered on the serious investigations of nanomaterials especially noble metal nanoparticles due to their exquisite sensitivity in chemical and biological sensing.¹⁵ Specifically, gold nanoparticles (AuNPs) exhibits enormous interest among researchers because they afford high surface-to-volume ratio for efficient and friendly loading of biomolecules, permit high and fast electron transfer between the electroactive species and the electrode. A great number of efficient synthetic procedures including chemical or photochemical reduction,¹⁶ electrochemical reduction,¹⁷ biosynthesis,¹⁸ etc., are being currently employed for the formation of AuNPs. In addition, the sonochemical method¹⁹ has proved to be a new route that has been receiving much interest and significance. It is intensively used technique in material chemistry for rapidly generating novel materials with useful properties having smaller size and higher surface area than other methods. Since the discovery of carbon nanotubes by Ijima²⁰ intense research has been prompted on the development of new one dimensional nanostructures that can be synthesized in the form of nanotubes (NTs), nanowires, nanorods etc. In the last decade, numerous publications have been

1
2
3 reported on the NTs of various kinds including carbon, metallic and polymeric. Furthermore,
4
5 NTs are found to be superior due to their blend of extraordinary properties such as nanometer
6
7 dimensions, elongated geometry, a defined cavity, possible control of the size and accessible
8
9 inner and outer surface.²¹ Various synthetic strategies such as hydrothermal synthesis, surfactant-
10
11 assisted synthesis, electroradiation have been established for the synthesis of NTs.²² Mitchell et
12
13 al, have pioneered a novel method called template synthesis for the production of nanotubes.²³
14
15 This method entails synthesizing the desired material within the pores of a nanoporous template
16
17 by chemical or electrochemical deposition or polymerization.²⁴ The formed nanostructures
18
19 (nanoparticles-nanotubes) which preserve the relevant morphological parameters are then
20
21 released from the porous matrix by template dissolution.
22
23
24
25
26

27
28 Concerning the advantageous characteristics of thiophene and its derivatives,
29
30 electrochemically or chemically generated polythiophene has been utilized in the development of
31
32 electrochemical sensor. The electropolymerization of thiophene does not require any oxidizing
33
34 or reducing agent and the film thickness can be maintained. Polythiophene (PTh) possess high
35
36 solubility, good conductivity ($10\sim 1000\text{ S cm}^{-1}$) and excellent thermal stability.²⁵ There is wide
37
38 spread realization that gold has high affinity to sulfur groups. The possibility of integrating gold
39
40 nanostructures with thiolated organic species i.e., inorganic-organic hybrid materials can provide
41
42 good chemisorptions that possess impressive analytical performances and these materials has
43
44 made significant strides in the application such as sensors and catalysis. A large amount of
45
46 research work has been devoted to gold nanoparticles modified thiophene composites.^{26,27}
47
48 However to best of our knowledge, electrochemical biosensor based on *Pp* CAT immobilized on
49
50 AuNPNTs-PTh hybrid has not been investigated before.
51
52
53
54
55
56
57
58
59
60

1
2
3
4
5
6
7
8
9
10
11
12
13
14
15
16
17
18
19
20
21
22
23
24
25
26
27
28
29
30
31
32
33
34
35
36
37
38
39
40
41
42
43
44
45
46
47
48
49
50
51
52
53
54
55
56
57
58
59
60

In this present research article, a simple bioelectrode has been proposed for the first time using CAT derived from *Pp* (CAT_{pp}) for the electrochemical detection of H₂O₂. Ultrasound irradiation was employed as a preparative protocol for the synthesis of gold nanoparticles, while the nanoporous alumina membrane was used as template for the fabrication of AuNPNTs. Then, the tubular nanostructures of gold were tethered onto the graphite (Gr) electrode via chemisorbed S-containing electropolymerized thiophene. The CAT_{pp} was immobilized onto the inorganic-organic hybrid (i.e., AuNPNTs-PTh) via EDC-NHS coupling reagent. The morphology and chemical composition of the developed biosensor Gr/PTh/AuNPNTs/EDC-NHS/CAT_{pp} have been investigated using SEM and EDX respectively. The electrochemical characterization of the electrodes was evaluated by CV and EIS technique. The analytical performance of the modified electrode was investigated using CV, DPV and chronoamperometry. Chronocoulometry was carried out for the determination of diffusion co-efficient of H₂O₂ on the bioelectrode. The proposed bioelectrode Gr/PTh/AuNPNTs/EDC-NHS/ CAT_{pp} explicitly demonstrates excellent electrocatalytic activity towards H₂O₂ with high sensitivity. The factors influencing the electrocatalytic response of the biosensor was examined. In addition, the interference of AA, UA and DA with reduction of H₂O₂ was studied at the Gr/PTh/AuNPNTs/EDC-NHS/CAT_{pp} electrode. The proposed bioelectrode is cost-effective with easy to fabricate and possesses long-term stability with anti-fouling properties.

2. Experimental section

2.1. Reagents and materials

The Yeast *Pp* (NCIM, no. 3419) was procured from National Collection of Industrial Micro-organism, NCL (Pune, India). Gold (III) chloride hydrate (HAuCl₄), Isopropanol, 3-Aminopropyl trimethoxysilane (APTMS), Sodium perchlorate (NaClO₄), EDC, NHS, Ascorbic

1
2
3 acid (AA), Doapmine (DA) and Uric Acid (UA) were obtained from Sigma-Aldrich. Thiophene
4
5 was purchased from Loba Chemie. 30% H₂O₂ and tri sodium citrate were purchased from Merck
6
7
8 Ltd., nanoporous alumina membrane (Anodisc, 0.2 μm) was obtained from Whatmann. PK-3
9
10 electrode polishing kit (0.05 mm aqueous polishing alumina and 1 mm polishing diamond) was
11
12 procured from BAS Inc. (Tokyo, Japan). Phosphate buffer saline (PBS) was prepared from stock
13
14 solution of 0.1 M K₂HPO₄, 0.1 M KH₂PO₄ and 0.1 M KCl. All other chemicals used were of
15
16 analytical reagent grade, unless otherwise mentioned, and were used without further purification.
17
18 The electrolyte solutions were deoxygenated during electrochemical experiments by bubbling
19
20 ultra-pure nitrogen for at least 10 min to make it a homogeneous mixture.
21
22
23

24 25 **2.2. Apparatus**

26
27 Electrochemical experiments such cyclic voltammetry (CV), differential pulse voltammetry
28
29 (DPV), chronoamperometry and electrochemical impedance spectroscopy (EIS) were performed
30
31 with Versa stat 3 (Princeton Applied Research, USA). Chronocoulometry (CC) experiment was
32
33 carried out using CH Instruments Inc. machine. The impedance spectra were further examined
34
35 by using a stimulated programme of Zsimp Win version 3.20. Ultrasound irradiation was
36
37 accomplished by using Q Sonica Ultrasonic processor equipped with Ti horn that enables to
38
39 generate 20 kHz ultrasound. The physical morphology of the modified electrodes were
40
41 characterized by scanning electron microscopy (SEM) and energy dispersive analysis of X-rays
42
43 (EDX) mapping using FE-SEM, model Hitachi S-4800 II with an accelerating voltage of 5 kV.
44
45 All the electrochemical experiments were carried out using conventional three electrode cell
46
47 assembly consisting of saturated calomel electrode (SCE) as the reference electrode, platinum
48
49 wire as the auxiliary electrode and bare Gr or CAT_{pp} modified electrode as working electrode.
50
51
52
53
54
55
56
57
58
59
60

2.3. Preparation of CAT_{pp} suspension

The *Pp* cells were sub-cultured on Malt Extract Yeast Peptone (MEYP) media at 28 °C containing malt extract 0.3 g, glucose 1 g, yeast extract 0.3 g, peptone 0.5 g, agar 2g, distilled water 100 mL, pH 6.4–6.8. The activity of CAT_{pp} was monitored spectrophotometrically by measuring every 15 sec at RT the decrease in absorbance at 240 nm caused by the degradation of H₂O₂ and using the molar extinction coefficient of 40.67 M⁻¹ cm⁻¹.²⁸ The assay mixture contained 50 mM PBS, 30 mM H₂O₂ and 50 μL of cell free extract in a total volume of 1 mL. The amount of enzyme required to degrade 1 μM of H₂O₂ per minute under standard conditions was defined as 1 enzyme unit of the CAT activity and the results were expressed in U (μM H₂O₂ min⁻¹ mL⁻¹). Consequently CAT_{pp} showed 24.6 U (in 50 μL of cell free extract) and it was chosen as model bioelectrocatalyst for the fabrication of our proposed biosensor. For the preparation of cell suspension, a loop-full of the inoculum was suspended in 1 mL of buffer solution of pH 7. Subsequently, it was subjected to ultrasonic disruption for about 5 min in order to remove the permeability barriers between the intracellular CAT enzyme and cell wall/membrane. The cell debris was removed by centrifugation and the supernatant was retained for the fabrication of the electrode.

2.4. Synthesis of AuNPs

AuNPs was prepared according to a reported sonochemical procedure^{29,30} with slight modification. In a typical procedure 0.05 g of HAuCl₄ was dissolved in 300 mL of distilled water hosted in a 500 mL beaker. In addition, 0.2 mM of isopropanol was also added to act as a radical scavenger and reaction accelerator. This solution was purged with Argon for about 20 min. to eliminate trace amounts of oxygen and to promote the radical formation (H• and OH•) from water. Subsequently, the solution was subjected to ultrasonication at room temperature, and then

1
2
3 3.4 g of tri sodium citrate was injected gradually to act as a stabilizing agent. The chemical
4
5 effects of ultrasound are derived principally from acoustic cavitations i.e., formation, growth and
6
7 implosive collapse of bubbles in the liquid. The collapse of such bubbles in the irradiated
8
9 solution results in localized hot spots with extremely high temperature (> 5000 K), pressure ($>$
10
11 20 M pa) and high cooling rates ($>10^7$ K s^{-1}) at a very short life time.³¹ In our preliminary
12
13 attempt to synthesize AuNPs by sonochemical method, the rate of reduction of an aqueous
14
15 solution of HAuCl_4 as a function of irradiation time and input amplitude of ultrasound was
16
17 determined. It was found that as the amplitude is increased from 10 to 100 at a rate of 20, the rate
18
19 of Au(III) reduction increases. However, it is apparent that at lower amplitude of ultrasound, the
20
21 sonochemical reduction is 20 times slower with the completion of formation of AuNPs is about 2
22
23 hours. Therefore amplitude of 100 was chosen as an optimum parameter for our experiment, in
24
25 which the formation of AuNPs requires only 5-10 min of irradiation time as witnessed by the
26
27 change in the colour of the gold solution. In order to obtain best results the sonication parameters
28
29 like amplitude of 100 that delivers an input power of ≈ 90 W were used. Upon ultrasonic
30
31 irradiation, the color of the irradiated solution changed from yellow to black and finally to
32
33 intense characteristic ruby red almost immediately within 5-10 min of the sonication process
34
35 indicating the formation of desired AuNPs.
36
37
38
39
40
41
42

43 **2.5. Synthesis of AuNPNTs**

44
45 In the first step, nanoporous alumina membrane was cleaned by means of ultrasonic bath in
46
47 isopropanol for about 3-5 times to make it free from any existing impurities. For the synthesis of
48
49 AuNPNTs, the nanoporous alumina membrane was modified with APTMS following a reported
50
51 literature³² and the as synthesized AuNPs solution was in-filtered by vacuum suction through the
52
53 amino derivatized pores of alumina membrane.²¹ Filling of the pores with AuNPs occurs
54
55
56
57
58
59
60

1
2
3 spontaneously. The silyl groups react with hydroxyl groups on the alumina membrane walls,
4
5 leaving the amine groups available for binding nanoparticles. 15 mL of AuNPs solution was
6
7 passed through the APTMS treated alumina membrane. It can be visually recognised that this
8
9 amount of solution coming out of the membrane is colourless indicating that all the AuNPs has
10
11 been strongly adsorbed onto the amino derivatized alumina template. We observed in our
12
13 experiments that passing additional amount of NPs solution through the membrane would appear
14
15 colored suggesting that the pore walls of the sacrificial template is covered with bound AuNPs
16
17 and there is no free space for binding of further AuNPs. After passing 15 mL AuNPs solution,
18
19 the template was washed by passing few mL of distilled water in order to ensure that the
20
21 membrane is not blocked. The AuNPNTs were isolated from the alumina membrane by
22
23 detaching the template via dissolution using 0.1 M NaOH for 3 hrs followed by centrifugation.
24
25 The isolated AuNPNTs was washed sequentially with distilled water and finally dried at 75 °C in
26
27 oven for 12 hrs. The so obtained AuNPNTs were dispersed to a final concentration of mg mL⁻¹ in
28
29 pure water and used for the fabrication of the bioelectrode.
30
31
32
33
34
35

36 **2.6. Preparation of bioelectrode**

37
38
39 An electrode was made by inserting a Gr rod of 6 mm diameter into a Teflon cylinder having the
40
41 same internal diameter and length of 6 cm. Electrical contact was established by inserting a
42
43 copper wire through the centre of Teflon cylinder. The surface of the Gr electrode was well
44
45 polished to obtain a mirror shiny surface using a PK-3 electrode polishing kit. It was then rinsed
46
47 for several minutes and ultrasonicated sequentially with distilled water to remove any impurities
48
49 followed by drying. Since the gold nanostructures can interact strongly with S-containing
50
51 functional group, the Gr surface was modified with a thin film of S-containing electroactive
52
53 thiophene monomer prepared by electropolymerization. In general, the analytical sensitivity and
54
55
56
57
58
59
60

1
2
3 reproducibility of any biosensor is determined by the surface of the modified electrode.
4
5 Therefore identification of optimum concentration of enzyme or thiophene is a crucial aspect for
6
7 the bioelectrode fabrication. The influence of electropolymerization parameters like the optimum
8
9 monomer concentration, the optimum number of CV cycles used to form polymer film and the
10
11 optimum scan rate of electropolymerization were investigated. As shown in the Fig.1 the best
12
13 results that presented maximum peak current and good peak profile in 0.5 M thiophene
14
15 concentration for 10 potential cycles at a scan rate of 50 mV s^{-1} were preferred for the
16
17 preparation of modified electrode. Then, the electropolymerization of thiophene on Gr electrode
18
19 was achieved by immersing the electrode in 10 mL of 0.5 M thiophene dissolved in acetonitrile
20
21 containing 0.12 g of NaClO_4 as the dopant. Subsequently it was subjected to cyclic scanning in
22
23 the range of 0 to -1.1 V at a scan rate of 50 mV s^{-1} for ten potential cycles which results in the
24
25 formation of thin films of PTh on Gr surface. The Gr/PTh electrode was rinsed with acetonitrile
26
27 to remove any unreacted monomer and then dried at room temperature. Then, 10 μL of
28
29 AuNPNTs solution was dropped uniformly onto the electrode surface and dried at room
30
31 temperature to obtain Gr/PTh/AuNPNTs modified electrode. Furthermore, in order to induce
32
33 covalent coupling between the CAT_{pp} solution and Au nanostructures, the electrode was
34
35 modified by drop coating 5 μL of 20 mM NHS solution and 5 μL of 40 mM EDC solution and
36
37 dried at room temperature. In addition to optimize the enzyme concentration, the current
38
39 response of the enzyme modified electrode was determined with different amounts of CAT
40
41 solution using CV. At low CAT concentration i.e., at 6 μL which is equal to 3 U, there was no
42
43 redox peaks detected with low peak current response whereas the best results with maximum
44
45 peak current were obtained with 5 U (10 μL) of enzyme concentration. However, further
46
47 increase in the enzyme concentration (10 U, 15 U and 20 U) results in a lower response
48
49
50
51
52
53
54
55
56
57
58
59
60

1
2
3 indicating diffusion problem. Therefore the ideal enzyme concentrations (10 μL) were chosen
4
5 for the fabrication of the bioelectrode. Finally covalent immobilization was carried out by
6
7 dropping 10 μL (approximately 5 U) of CAT_{pp} suspension onto the electrode followed by
8
9 incubating at 4 $^{\circ}\text{C}$ for 30 min. The resultant Gr/PTh/AuNPNTs/EDC-NHS/ CAT_{pp} bioelectrode
10
11 was rinsed with pure water to remove any unbound or loosely attached CAT_{pp} and appropriately
12
13 used for the electrochemical detection of H_2O_2 . For comparison, Gr/EDC-NHS/ CAT_{pp} and
14
15 Gr/PTh/EDC- NHS/ CAT_{pp} electrodes were prepared in a similar fashion.
16
17
18
19

20 21 **3. RESULTS AND DISCUSSION**

22 23 **3.1. Structural characterization of AuNPs using UV-Vis spectroscopy, XRD and SEM**

24
25 The UV-Vis spectrophotometric analysis was carried using Shimadzu 1700 UV-Vis
26
27 spectrophotometer. The UV-Vis spectra recorded for the sonochemically reduced AuNPs is
28
29 given in the Fig. 2A. It can be seen that a Surface Plasmon resonance (SPR) band centred at 520
30
31 nm is observed indicating the successful formation of AuNPs. In addition, it is well documented
32
33 in literature that SPR band for spherical AuNPs usually occurs in the range between 520 and
34
35 530 nm.³³ This result suggests that spherical AuNPs were typically formed in our synthesis
36
37 procedure. To investigate the size and crystalline structure of AuNPs, X-ray diffraction
38
39 measurement was carried out. The powder XRD pattern (Fig. 2B) showed the appearance of
40
41 sharp peaks at 2θ value 38.1, 44.3 and 64.5 indexed to the Au (111), (200), (220) planes
42
43 respectively that can be assigned to the Face-centred cubic structure of gold.³⁴ No other peaks
44
45 characterized for the impurities can be observed elucidating the purity of the AuNPs.
46
47 Furthermore, the particle size calculated for the crystalline nanoparticles using Debye-Scherrer
48
49 equation was found to be 13.8 nm. The scanning electron micrograph of AuNPs as shown in Fig. 2C
50
51 exhibits many spherical particles. It can be recognized that AuNPs are evidently individual
52
53
54
55
56
57
58
59
60

1
2
3 entities. The particle size analysis of AuNPs was performed using ImageJ software and the
4
5 average diameter was found to be of 10 nm as illustrated in Fig. 2D. From, these results it can be
6
7 explained that the shape of ultrasonically prepared AuNPs is found be spherical and its average
8
9 particle diameter is 10 ± 2 nm.
10
11

12 13 14 **3.2 Physical characterization of the modified electrodes using SEM and EDX**

15
16 Fig. 3A shows the SEM image of a small piece of alumina template containing AuNPs before
17
18 dissolution. It is seen that many AuNPs adhere to the porous template throughout the entire
19
20 surface. Furthermore, the AuNPs synthesized by the sonochemical method were almost spherical
21
22 in shape. This SEM image validates the highly ordered arrangement of AuNPs within the pores
23
24 of the templates leading to the formation of AuNPNTs. The Gr/PTh/AuNPNTs modified
25
26 electrode shows the existence of tubular morphology (Fig. 3A inset) formed as a resultant of
27
28 sacrificial templates. It can be observed that the diameter of the AuNPNTs is ca. 200 nm. From
29
30 the inset of Fig. 3A one can speculate the homogenous distribution of AuNPNTs in the electrode
31
32 composite. This elucidates that PTh provides a suitable surface for the adherence of AuNPNTs
33
34 onto the Gr surface via S-Au chemisorptions. Comparatively, the SEM image of
35
36 Gr/PTh/AuNPNTs/EDC-NHS/CAT_{pp} electrode (Fig. 3B) reveals the presence of several bright
37
38 globular discrete particles. These particles can be attributed to the successful immobilization of
39
40 large amounts of CAT_{pp} on the void of porous AuNPNTs structures via EDC-NHS covalent
41
42 coupling. The high surface coverage area and biocompatibility of AuNPNTs provides a good
43
44 platform for the immobilization of large amounts of CAT_{pp}.
45
46
47
48
49
50

51
52 An elemental analysis was carried out to comprehend the chemical properties of the
53
54 composites. The investigation of nanoporous alumina membrane filled with AuNPs by EDX
55
56 (Fig. 3C) revealed the presence of elemental Au, Al, Si, C and O signals. The Al, Si, signals may
57
58
59
60

1
2
3 be attributed to the alumina template. While, the EDX data obtained for Gr/PTh/AuNPNTs
4 electrode (Fig. 3D) shows the S signal arising from the thiophene despite of Au, C and O. This
5 gives an indication of S-Au chemisorptions. However the Gr/PTh/AuNPNTs/EDC-NHS/CAT_{pp}
6 (Fig. 3E) illustrates a similar trend in the composition with the presence of Au, S, C and O along
7 with Fe anticipated for the CAT_{pp}. The detailed data of weight percentage of the elements
8 measured for each modified electrodes are tabulated at the top of the insets of the corresponding
9 Fig. 3C-E.

10 11 12 13 14 15 16 17 18 19 20 21 22 23 24 25 26 27 28 29 30 31 32 33 34 35 36 37 38 39 40 41 42 43 44 45 46 47 48 49 50 51 52 53 54 55 56 57 58 59 60

3.3. Electrochemical characterization of the bioelectrode by CV and EIS using potassium ferricyanide

To investigate the ion accessibility of the modified electrodes, CVs of bare Gr, Gr/PTh, Gr/PTh/AuNPNTs and Gr/PTh/AuNPNTs/EDC-NHS/CAT_{pp} were obtained using 5 mM Fe(CN)₆^{3-/4-} as electrochemical probe. It is clear from the Fig. 4A, that the redox current at the Gr/PTh (curve b) was superior to that of bare Gr (curve a) which may be due to the good conductivity of PTh that can improve the electron transfer rate. When the electrode was modified further with AuNPNTs, the Gr/PTh/AuNPNTs electrode exhibited highest peak current indicating that the AuNPNTs can act as tiny conducting centers accelerating the electron transfer and correspondingly enhanced active electrode surface area. This validates the improved S-Au chemisorptions formed between the inorganic and organic hybrid. However the redox current decreased obviously after CAT_{pp} immobilization (curve d) indicating the sluggish electron transfer at the electrode surface due to the presence of insulating enzyme layer. This proves the higher steric hindrance and successful immobilization of the enzyme in the nanocomposite. In addition, the peak to peak separation (ΔE_p) between the anodic and cathodic peaks was found to be bare Gr; ($\Delta E_p=172$ mV) > Gr/PTh ($\Delta E_p=169$ mV) > Gr/PTh/AuNPNTs ($\Delta E_p=141$ mV) and

1
2
3 Gr/PTh/AuNPNTs/EDC-NHS/CAT_{pp} ($\Delta E_p=149$ mV). Besides, the voltammetric profiles (Fig.
4
5 4A) were subjected to quantitative mathematical analysis to elucidate the electroactive surface
6
7 area. The active electrode area can be calculated according to Randles-Sevick equation as
8
9 follows³⁵

$$I_p = 2.69 \times 10^5 AD^{1/2} n^{3/2} v^{1/2} C \quad (1)$$

14
15 where I_p is the peak current of the redox couple, A is the area of the electrode (cm^2), D is the
16
17 diffusion co-efficient ($\text{cm}^2 \text{s}^{-1}$), n is the number of electrons participating in the redox reaction, v
18
19 is the scan rate (V s^{-1}) and C is the concentration of the probe molecule in the bulk solution
20
21 (mol cm^{-3}). The calculated electroactive surface area was found to be bare Gr (0.167 cm^2) <
22
23 Gr/PTh (0.175 cm^2) < Gr/PTh/AuNPNTs (0.231 cm^2) > Gr/PTh/AuNPNTs/EDC-NHS/CAT_{pp}
24
25 (0.211 cm^2). It can be seen that the electroactive surface area of Gr/PTh/AuNPNTs electrode
26
27 increased about 38.32% and 32% compared to that of bare Gr and Gr/PTh respectively which
28
29 justifies the higher peak current achieved from the Gr/PTh/AuNPNTs electrode and validates the
30
31 effective evidence for the superior conductivity of AuNPNTs as expected.
32
33
34
35

36
37 In addition, EIS experiments were also carried out for probing the features of the electrode
38
39 surface during each step wise construction of the biosensor. As widely used EIS is more
40
41 consistent, efficient and precise than CV. A typical impedance spectrum represented in the form
42
43 of Niquist plots consists of a semi circle part and a linear part corresponding to electron transfer
44
45 limited process and diffusion limited process respectively. As shown in Fig. 4B, the redox
46
47 process at the modified electrodes is controlled by both diffusion and electrochemical reactions.
48
49 The diameter of the semicircle portion observed at higher frequency range is equivalent to the
50
51 electron transfer resistance R_{ct} . Its value can be used as a direct and sensitive parameter to depict
52
53 the interfacial properties of surface-modified electrodes. The EIS experimental data obtained for
54
55
56
57
58
59
60

1
2
3 the bare Gr (a), Gr/PTh (b), Gr/PTh/AUNPNTs (c) and Gr/PTh/AUNPNTs/EDC-NHS/CAT_{pp} (d)
4
5 at frequencies varying from 0.1 Hz to 100 kHz are compared with an equivalent circuit (inset of
6
7 Fig. 4B) that assists to comprehend the electrical properties of the electrode/solution interface. It
8
9 is noticeable that the circuit is composed of elements like solution resistance (R_s), double layer
10
11 capacitance (C_{dl}), faradic resistance (R_f), Warburg impedance (W) and R_{ct} . The best fitted
12
13 impedance data obtained using the equivalent circuit is tabulated in Table 1. From the Fig. 4B, it
14
15 can be perceived that the bare Gr electrode (curve a) manifested a large semicircle implying a
16
17 high R_{ct} (65.92 Ω) of the redox probe which can be attributed to the poor catalytic activity of the
18
19 Gr electrode. On the other hand, the Gr/PTh electrode depicts an R_{ct} of 52.34 Ω which was
20
21 reflected by the decreased semicircle part. This is apparently due to the amelioration of electric
22
23 conductivity by the polymer. Comparatively, after modification with AuNPNTs, the diameter of
24
25 the semi-circle part was found to decrease gradually with R_{ct} of 41.38 Ω . This provides the
26
27 evidence that the incorporation of AuNPNTs results in excellent electrical conductivity. In
28
29 contrast, the CAT_{pp} modified bioelectrode showed hindered electron transfer with an increase in
30
31 the R_{ct} value of 44.73 Ω which is in-turn reflected by the increased semi-circle part suggesting
32
33 the presence of CAT_{pp} can block the electron transfer kinetics which was consistent with the CV
34
35 results indicating the successful immobilization of CAT_{pp}.
36
37
38
39
40
41
42

43 Further it is well known that the electron transfer rate (k^0) for the ferricyanide system at the
44
45 electrode surface decreases with the increase in the ΔE_p value.³⁶ Therefore k^0 was calculated
46
47 using the following equation
48
49

$$R_{ct} = R.T / (n.F)^2 A . k^0 . C \quad (2)$$

50
51
52 Where R_{ct} is the electron transfer resistance from the corresponding impedance plots of the
53
54 modified electrodes, R is the ideal gas constant, T is the temperature, F is faraday constant, A is
55
56
57
58
59
60

1
2
3 the area of the electrode, C is the molar concentration of the $\text{Fe}(\text{CN})_6^{3-/4-}$. From the equation (2),
4
5 the k^0 for the bare Gr, Gr/PTh, Gr/PTh/AuNPNTs and Gr/PTh/AuNPNTs/EDC-NHS/ CAT_{pp}
6
7 modified electrodes were found to be 2.78×10^{-4} , 3.5×10^{-4} , 4.4×10^{-4} and $4.1 \times 10^{-4} \text{ cm s}^{-1}$
8
9 respectively. The k^0 for Gr/PTh/AuNPNTs electrode was found to be 58% times higher than bare
10
11 Gr electrode and 26% times higher than Gr/PTh electrodes in the same electrolyte solution
12
13 indicating that the presence of AuNPNTs improved the conductivity and increased the electron
14
15 transfer rate.
16
17
18
19

20 **3.4 Comparison of voltammetric response of the modified electrodes towards H₂O₂** 21 **reduction** 22 23

24 To verify the efficacy of the proposed bioelectrode towards the detection of H_2O_2 , the
25 electrochemical reduction at the Gr/PTh/AuNPNTs/EDC-NHS/ CAT_{pp} electrode was examined
26 and compared with the other modified electrodes. Fig. 5A illustrates the CV results measured in
27 nitrogen saturated solution in presence of 4 mM H_2O_2 in the potential window 0 to -0.8 V at a
28 scan rate of 50 mV s^{-1} . As can be seen, the current delivered at the Gr/EDC-NHS/ CAT_{pp} (curve
29 a) is very small indicating the lack of stable electroactive species. However under the identical
30 conditions, Gr/PTh/EDC-NHS/ CAT_{pp} (curve b) produced increased peak current giving a clear
31 evidence for the better conductivity, larger surface area and good electrocatalytic activity of PTh
32 towards H_2O_2 . In presence of AuNPNTs without CAT_{pp} , there is a significant increment in the
33 reduction current (curve c, Gr/PTh/AuNPNTs electrode) than that of the earlier two electrodes
34 which validates the effective surface area of the electrode is efficiently enhanced by the use of
35 Au nanostructures composite. Prior to immobilization of CAT_{pp} onto the inorganic-organic
36 hybrid (i.e, AuNPNTs and PTh) we examined the superiority of AuNPNTs over AuNPs. To
37 support the information, CVs were recorded for Gr/PTh/AuNPs (a') electrode in presence of
38
39
40
41
42
43
44
45
46
47
48
49
50
51
52
53
54
55
56
57
58
59
60

1
2
3 2 mM H₂O₂ and compared with Gr/PTh/AuNPNTs (b'). It is clear from the inset of Fig. 5A that
4
5 the Gr/PTh/AuNPNTs electrode demonstrates better electrocatalytic activity (ca. 1.5 fold
6
7 increased current) towards H₂O₂ due to their high surface to volume ratio than that of AuNPs,
8
9 which acts as a tiny conducting wires and offers more binding sites for the molecules allowing
10
11 the loading of large number of enzyme molecules thus enhances the electrocatalytic response of
12
13 H₂O₂. Whilst the proposed bioelectrode (curve d) showed 1.5 fold higher electrocatalytic
14
15 response to H₂O₂ than AuNPNTs modified electrode and 2.4 fold higher current response than
16
17 PTh modified electrodes at more positive potential. Apparently, the Gr/PTh/AuNPNTs/EDC-
18
19 NHS/CAT_{pp} displayed a pair of quasi-reversible redox peaks of Fe^(III)/Fe^(II) redox couple
20
21 characteristic of the CAT with formal potential E^0 -0.322 V which was found to be slightly
22
23 positive than -0.414 V reported for SWCNTs-Au modified electrode with CAT.³⁷ This positive
24
25 shift in the E^0 can be due to the components of the electrode that affects the electrostatic double
26
27 layer. Based on these experimental observations we can interpret that AuNPNTs acts as an
28
29 electron transfer facilitator from the redox species of CAT to the electrode surface. The tubular
30
31 gold nanostructures assist to accommodate more number of CAT molecules in favorable
32
33 orientation at the vicinity of the electrode. The integration of AuNPNTs-PTh (inorganic-organic
34
35 hybrid) improves the conductivity, lowers the over potential for H₂O₂ reduction and offers a
36
37 biocompatible micro-environment for CAT_{pp}. Accordingly, it is noteworthy to declare that
38
39 CAT_{pp} (where only 5 U of enzyme has been used) can be a good preference for the fabrication of
40
41 H₂O₂ sensor which is superior than reported literature of 200 U of CAT from bovine liver.³⁸
42
43
44
45
46
47
48
49
50
51
52
53
54
55
56
57
58
59
60

3.5. Determination of Diffusion coefficient and adsorption of H₂O₂ on the Gr/PTh/AuNPNTs/EDC-NHS/CAT_{pp} bioelectrode using CC

Chronocoulometry is one of the most conventional electrochemical techniques used in electroanalytical chemistry. It is the measurement of charge as a function of time. The CC technique was applied to determine diffusion co-efficient (D) and Q_{ads} of H₂O₂ on the proposed electrode using Anson equation³⁹

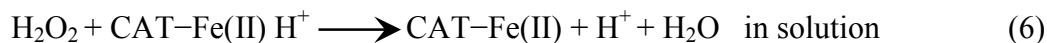
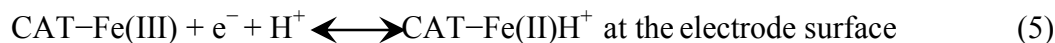
$$Q = \frac{2nFACDt^{1/2}}{\pi^{1/2}} + Q_{\text{dl}} + Q_{\text{ads}} \quad (3)$$

Where n represents the number of electrons transferred in the electrochemical reaction, F is the faraday constant, A is the area of the electrode in cm², D is the diffusion co-efficient (cm² s⁻¹), t is the time (ms), Q_{dl} is the double layer charge and Q_{ads} is the adsorption charge. Two series of CC experiments were performed, first using the Gr/PTh/AuNPNTs/EDC-NHS/CAT_{pp} electrode in presence of 2 mM H₂O₂ and then the same electrode in the supporting electrolyte in absence of electroactive species. Typical CC responses i.e., plot of charge as a function of time is given in Fig. 5B. The CC responses of the modified electrode in presence and absence of H₂O₂ was then converted to Anson plots by plotting Q vs. $t^{1/2}$. The Anson plot shows a linear relationship of Q upon $t^{1/2}$ indicating a diffusion controlled electrochemical process. From the slope and intercept of the linear relationship the parameters D and Q_{ads} was calculated using the above equation (3). Accordingly, D and Q_{ads} was estimated to be 6.1×10^{-5} cm² s⁻¹ and 6.69×10^{-5} C. In addition the surface concentration Γ_s was calculated using the equation (4) and it was found to be 12.5×10^{-10} mol cm⁻².

$$\Gamma_s = \frac{Q_{\text{ads}}}{nF} \quad (4)$$

3.6. Electrocatalytic properties of H₂O₂ biosensor

The electrocatalytic reduction of H₂O₂ at the proposed bioelectrode was studied in the absence and presence of varying concentration of the analyte in 0.1 M PBS (pH 7). Fig. 6A shows CVs obtained in the potential window 0 to -0.8 V at a scan rate of 50 mV s⁻¹. In the absence of H₂O₂, pair of redox peaks were observed at -0.252 V (*E*_{pa}) and -0.370 V (*E*_{pc}) respectively is characteristic Fe^(III)/Fe^(II) redox couple of CAT. Upon sequential addition of 1 mM H₂O₂, the voltammetric peak corresponding to the electrocatalytic reduction of H₂O₂ increases gradually at -0.370 V accompanied by the decrease of oxidation current indicating a typical electrocatalytic process at the Gr/PTh/AuNPNTs/EDC-NHS/CAT_{pp} electrode. After addition of twofold concentration of H₂O₂ the cathodic peak was found to increase correspondingly suggesting that the catalytic current of the bioelectrode was determined by the concentration of H₂O₂. The electrocatalytic mechanism can be expressed as follows.



Here, CAT-Fe(III) and CAT-Fe(II) represent the oxidized and reduced form of CAT respectively. From the mechanism, it can be seen that when CAT-Fe(III) undergoes electron transfer reaction with the electrode, CAT-Fe(II)H⁺ can be oxidized by H₂O₂ in the solution to regenerate CAT-Fe(III). This above electrode reaction slightly differs from conventional E_rC_i' mechanism in that both CAT-Fe(III) and CAT-Fe(II)H⁺ are surface confined. A typical calibration plot of electrocatalytic current versus concentration of H₂O₂ for Gr/PTh/AuNPNTs/EDC-NHS/CAT_{pp} electrode is shown in Fig. 6A Inset. As revealed in the inset, the cathodic peak current (*I*_{pc}) was found to be linear with concentrations of H₂O₂ in the range 0 to 8 mM and its linear regression equation is as given below

$$I_{pc} = -5.805 \times 10^{-5} - 5.927 \times 10^{-5} C_{H_2O_2} \text{ (mM)}; R = -0.990 \quad (7)$$

Differential Pulse Voltammetry (DPV) has the advantage of having higher current sensitivity and better resolution compared to CV. Therefore, the detection of various concentrations of H₂O₂ using the proposed electrode was investigated using DPV in the potential range 0 to -0.8 V. As for the CV analysis, DPV measurements were first obtained in absence of H₂O₂, followed by analysis of increasing concentrations of H₂O₂. It is apparent from the Fig. 6B that the dependence of reduction peak current was found to be linear (inset Fig. 6B) with the concentration of H₂O₂ in the range 0 to 6 mM. The linear regression equation is as follows

$$I_{pc} = -7.270 \times 10^{-4} - 7.085 \times 10^{-4} C_{H_2O_2} \text{ (mM)}; R = -0.997 \quad (8)$$

To elucidate the kinetics of electrode reaction of H₂O₂ detection at the electrode surface, the effect of scan rate on the peak current at the modified electrode was investigated using 2 mM H₂O₂ and the results are shown in Fig. 6C. As expected, the overlaid CVs of the Gr/PTh/AuNPNTs/EDC-NHS/CAT_{pp} electrode illustrated an increase in oxidation and reduction peak current with the increase of scan rate from 25 to 300 mV s⁻¹. A good linear relationship between the peak currents and square root of scan rate was achieved as shown in the inset of Fig. 6C with the linear regression equation as specified below

$$I_{pa} = 7.672 \times 10^{-6} + 5.629 \times 10^{-7} v^{1/2} \text{ (V s}^{-1}\text{)}; R = 0.995 \quad (9)$$

$$I_{pc} = -5.529 \times 10^{-5} - 8.660 \times 10^{-7} v^{1/2} \text{ (V s}^{-1}\text{)}; R = -0.995 \quad (10)$$

All these characteristics suggested that the electrochemical reaction occurring at the Gr/PTh/AuNPNTs/EDC-NHS/CAT_{pp} electrode is a diffusion controlled process.

3.7. Influence of applied potential, temperature and pH on Gr/PTh/AuNPNTs/EDC-NHS/CAT_{pp} bioelectrode

To improve the performance of the biosensor an assortment of working parameters such as applied potential, temperature and pH that play an important role were optimized.

The selection of the operating potential on the working electrode is useful in achieving high sensitivity, best detection limit and good selectivity of the system avoiding electroactive interfering species. In order to evaluate the effect of applied potential, the electrocatalytic reduction of H₂O₂ was examined at the Gr/PTh/AuNPNTs/EDC-NHS/CAT_{pp} electrode by chronoamperometry over the potential range -200 to -450 mV. Amperometric measurements were recorded in stirring conditions by sequentially injecting 2 mM H₂O₂ for a period of 300 s. Fig. 7A shows a plot of operating potential vs. electrocatalytic peak current response to the successive addition of H₂O₂. As can be seen, during the potential range studied we can interpret that the reduction of H₂O₂ initiates at -200 mV and increases appreciably towards negative potential reaching a plateau at -350 mV. However with more negative increase in potential, the peak current decreased revealing that the proposed electrode has better electrocatalytic activity for the reduction of H₂O₂ at -350 mV. Consequently to achieve the highest sensitivity and to avoid interferences an applied potential of -350 mV (vs. SCE) was chosen for all further experiments.

Furthermore we have investigated the effect of temperature on the biocatalytic response of the bioelectrode by CV in presence at a constant H₂O₂ concentration of 2 mM. Fig. 7A shows the trend of the variation of electrocatalytic peak response of the Gr/PTh/AuNPNTs/EDC-NHS/CAT_{pp} electrode as a function of temperature. As depicted, by increasing the temperature from 10 °C, the catalytic current increases to achieve its maximum value at 70 °C. A decrease in

1
2
3 current can be observed when the temperature exceeds 70 °C indicating partial denaturation of
4 the enzyme at higher temperature. This increase in thermal stability can be attributed to
5 beneficial effect brought by AuNPNTs-PTh hybrid that provides good biocompatibility to the
6 immobilized enzyme. Nevertheless, considering the life time and characteristic electrocatalytic
7 response of the bioelectrode, all subsequent experiments were performed at room temperature.
8
9

10 To determine the pH stability of the Gr/PTh/AuNPNTs/EDC-NHS/CAT_{pp} electrode, the
11 dependence of the solution pH on the voltammetric response of the bioelectrode was scrutinized
12 in the pH range 3 to 10 (standard buffer solutions) in presence of constant H₂O₂ concentration of
13 2 mM. According to the pH profile depicted in Fig. 7B, the peak current enhances with an
14 increasing pH reaching a maximum at pH 7 and declines afterwards until pH 10. Consequently,
15 pH 7 was chosen as optimum pH with maximum activity of the enzyme constituents
16 immobilized on the bioelectrode which is consistent with the reported literature⁴⁰ indicating that
17 the electrode composite offers a biocompatible micro-environment for CAT.
18
19

20 **3.8. Chronoamperometric response of the Gr/PTh/AuNPNTs/EDC-NHS/CAT_{pp}** 21 **bioelectrode** 22 23

24 The chronoamperometric current response of the proposed bioelectrode was measured in 0.1 M
25 nitrogen saturated PBS solution under the optimal experimental conditions. Fig. 8A illustrates a
26 typical current versus time plot of Gr/PTh/AuNPNTs/EDC-NHS/CAT_{pp} electrode that was
27 evaluated on stepwise addition of various aliquots of H₂O₂ to stirring electrolyte solution at a
28 static potential of -350 mV (vs. SCE). A rapid co-relative amperometric current response ca. 7s
29 was attained at every 30 s aliquots of H₂O₂ addition indicating a fast electron transfer. From the
30 steady state amperograms a calibration plot was made by using current as a function of
31 concentration and the results are shown in Fig. 8A inset. The electrode exhibited a wide linear
32
33

1
2
3 range between 0.05 mM to 18.5 mM with a correlation co-efficient of -0.991 , detection limit
4
5 0.12 μM (at a signal to noise ratio of 3) and sensitivity of $26.2 \text{ mA mM}^{-1} \text{ cm}^{-2}$. At higher
6
7 concentration range, the electrocatalytic response of the bioelectrode tends to become a plateau
8
9 illustrating a characteristic Michaelis–Menten kinetic mechanism. The Michaelis–Menten
10
11 constant (K_M) gives an indication of enzyme-substrate kinetics and can be estimated from the
12
13 electrochemical analogue of Line-weaver-Burk equation⁴¹ as follows
14
15

$$1/I_{ss} = 1/I_{max} + K_M/I_{max} \cdot C \quad (11)$$

16
17
18 Where I_{ss} is the steady state current after the addition of the substrate, C is the bulk
19
20 concentration of the substrate and I_{max} is the maximum current measured under saturated
21
22 substrate condition. From the plot of $1/I_{ss}$ vs. $1/C$ the K_M value can be estimated using the slope
23
24 and intercept for the proposed bioelectrode. The K_M value for the Gr/PTh/AuNPNTs/EDC-
25
26 NHS/CAT_{pp} electrode was calculated to be 1.4 mM that was lesser than 40.7 mM for CAT
27
28 immobilized on a GCE by poly(glycidyl methacrylate-co-vinylferrocene)⁴² signifying the good
29
30 enzyme activity, strong binding of the immobilized CAT_{pp} on AuNPNTs-PTh composite and its
31
32 high affinity towards H_2O_2 detection. The beneficial analytical characteristics of our proposed
33
34 bioelectrode was compared with other previously reported non enzymatic, HRP and CAT based
35
36 H_2O_2 sensors^{38,42–46} and presented in Table 2. As summarized in the table, the
37
38 Gr/PTh/AuNPNTs/EDC-NHS/CAT_{pp} electrode displayed superior analytical data to those
39
40 documented in the literature.
41
42
43
44
45
46
47

48 **3.9. Effect of interferences on Gr/PTh/AuNPNTs/EDC-NHS/CAT_{pp} bioelectrode**

49
50 To fulfill the practical applicability of the biosensor the selectivity study is obligatory for any
51
52 developed biosensors. The influences of some of the common electroactive species that are
53
54 accredited to interfere with H_2O_2 detection have been investigated as shown in Fig. 8B. The low
55
56
57
58
59
60

operating potential -350 mV (vs. SCE) afforded by the Gr/PTh/AuNPNTs/EDC-NHS/CAT_{pp} electrode significantly curtails the effect of interferents such as AA, UA and DA which are commonly present in biological samples. The normal concentration ranges of AA, UA and DA are $34\text{--}79$ mM, $0.18\text{--}0.42$ mM and 1 μM respectively.⁴⁷ The amperometric response obtained in presence of 2 mM H₂O₂ (a) shows a well defined stable current response. However, on the contrary the contributions of subsequent addition of 200 μM DA (b), 1 mM AA (c) and 0.5 mM UA (d) higher than the normal physiological concentration are very negligible indicating that Gr/PTh/AuNPNTs/EDC-NHS/CAT_{pp} electrode has good selectivity for H₂O₂. The integration of AuNPNTs-PTh (inorganic-organic hybrid) lowers the over potential for H₂O₂ reduction and allows us to surmount the potential interference.

3.10. Stability and reproducibility test for Gr/PTh/AuNPNTs/EDC-NHS/CAT_{pp} bioelectrode

The repeatability, stability and reproducibility of the Gr/PTh/AuNPNTs/EDC-NHS/CAT_{pp} bioelectrode are essential factors for its practical application. The repeatability of the proposed bioelectrode was investigated by a series of repetitive measurements carried out with the same modified electrode in presence of 3 mM H₂O₂ in nitrogen saturated 0.1 M PBS solution. The results of 21 successive CV measurements showed that the bioelectrode could retain 95% of its initial current response indicating that the modified bioelectrode had good repeatability and ability to prevent the electrode from fouling. Further the long-term stability (shelf life) was also tested for 4 week period. The electrocatalytic response of the fabricated electrode was verified by consecutive potential scans in presence of 2 mM H₂O₂. The magnitude of the current response measured under identical conditions decreased ca. 1.2% of its initial value after one week and 4.2% in four weeks representing that the electrode was stable towards H₂O₂ detection. The

1
2
3 bioelectrode was cleaned with CV cycles in PBS after each measurement to eradicate the
4
5 adsorption of the analyte and preserved at 4 °C. In addition, the electrode capability to generate a
6
7 reproducible surface was also examined using six different modified electrodes fabricated using
8
9 the same procedure. These six electrodes exhibited analogous electrocatalytic response to 3 mM
10
11 H₂O₂ with RSD of 3.1 % obtained in optimum conditions which validated that reproducible
12
13 results can be obtained using the Gr/PTh/AuNPNTs/EDC-NHS/CAT_{pp} bioelectrode. These
14
15 results demonstrate that the proposed bioelectrode has good repeatability, high stability and
16
17 admirable reproducibility which may be ascribed to the excellent biocompatible micro-
18
19 environment offered by the AuNPNTs-PTh (inorganic-organic hybrid) that conserves CAT_{pp}
20
21 from antifouling and denaturation.
22
23
24
25

26 27 **4. CONCLUSION**

28
29 In an effort to develop a highly sensitive electrochemical H₂O₂ biosensor, we present the use
30
31 of CAT_{pp} as a bioelectrocatalyst in the fabrication of a sensor. We have successfully synthesized
32
33 AuNPs through sonochemical reduction of HAuCl₄⁻. The template synthesis method assisted us
34
35 to prepare AuNPNTs that offers high surface area to volume ratio. The modification of the Gr
36
37 surface with electropolymerized film of thiophene provided S groups that allow strong binding
38
39 of AuNPNTs onto the Gr surface. The integration of S-Au affords an effective immobilization
40
41 platform to fabricate a novel H₂O₂ biosensor. Investigations of the modified electrode evidently
42
43 revealed that the proposed electrode showed enhanced electrocatalytic activity towards H₂O₂
44
45 reduction at a potential of ca -350 mV (vs. SCE) less positive than the bare Gr electrode. The
46
47 biosensor possesses the function of AuNPNTs and PTh that can facilitate electron transfer,
48
49 accommodate more number of enzyme molecules, provide biocompatible micro-environment,
50
51 lower the reduction potential and improve the conductivity. Furthermore, the AuNPNTs-PTh
52
53
54
55
56
57
58
59
60

1
2
3 modified CAT_{pp} immobilized bioelectrode illustrates some of the excellent characteristics like
4 rapid response, wide linear range, low detection limit, excellent selectivity, good repeatability,
5
6 long-term stability, admirable reproducibility, anti-fouling properties, low cost with easy
7
8 fabrication. It can be concluded from the experimental results, that the proposed bioelectrode
9
10 could be an alternative to existing expensive enzymatic methods for the detection of H_2O_2 .
11
12
13
14

15 **Acknowledgements**

16
17 The authors gratefully acknowledge the financial assistance from the Department of Atomic
18 Energy – Board of Research in Nuclear Sciences, Government of India. We also thank Sri.
19
20 A.V.S. Murthy, honorary secretary, Rashtreeya Sikshana Samiti Trust, Bangalore and Dr Shanta
21
22 Sastry, Principal, N.M.K.R.V. College for Women, Bangalore for their continuous support and
23
24 encouragement. Part of this work was supported by the DGIST R&D Program of the Ministry of
25
26 Education, Science and Technology of Korea (14-BD-01).
27
28
29
30
31
32
33
34
35
36
37
38
39
40
41
42
43
44
45
46
47
48
49
50
51
52
53
54
55
56
57
58
59
60

References

- 1 A. Salimi, R. Hallaj, S. Soltanian and H. Mamkhezri, *Anal. Chim. Acta*, 2007, **594**, 24–31.
- 2 Y. Usui, K.Sato and M. Tanaka, *Angew. Chem. Int. Ed.*, 2003, **42**, 5623–5625.
- 3 C.D. Bryan and J.C. Christopher, *J. Am. Chem. Soc.*, 2008, **130**, 11561–11561.
- 4 W.P. Lian, L. Wang, Y.H. Song, H.Z. Yuan, S.C. Zhao, P. Li and L.L. Chen, *Electrochim Acta*, 2009, **54**, 4334–4339.
- 5 B. Wang, J. J. Zhang, Z. Y. Pan, X. Q. Tao and H.S. Wang, *Biosens. Bioelectron.*, 2009, **24**, 1141–1145.
- 6 L. Wenjuan, Y. Ruo, C. Yaqin, Z. Lu, C. Shihong and L. Na, *J. Biochem. Biophys. Meth.*, 2008, **70**, 830–837.
- 7 S. Nalini, S. Nandini, S. Shanmugam, S.E. Neelagund, J.S. Melo and G.S. Suresh, *J. Solid State Electrochem.*, 2014, **18**, 685–701.
- 8 L.Zhang, *Biosens. Bioelectron.*, 2008, **23**, 1610–1615.
- 9 X. Miao, R.Yuan, Y. Chai, Y. Shi and Y. Yuan, *J. Electroanal. Chem.*, 2008, **612**, 157–163.
- 10 X. Zeng, W.Weiz, X. Li, J. Zheng and L. Wu, *Bioelectrochemistry*, 2007, **71**, 135–141.
- 11 M. Veenhuis and J. Goodman, *J. Cell Sci.*, 1990, **96**, 583–590.
- 12 P.E. Purdue and P.B. Lazarow, *Annu. Rev. Cell Dev. Biol.*, 2001, **17**, 701–752.
- 13 D. Koleval, V. Petroval, T. Hristozova and A. Kujumdzieva, *Biotechnol. Biotechnol. Equip.*, 2008, **22**, 762–768.
- 14 I.J. Van-der-Klei, H. Yurimoto, Y. Sakai and M. Veenhuis, *Biochim. Biophys. Acta*, 2006, **1763**, 1453–1462.
- 15 A. Moores and F. Goettmann, *New J. Chem.*, 2006, **30**, 1121–1132.
- 16 J. Polte, T.T. Ahner, F. Delissen, S. Sokolov, F. Emmerling, A.F. Thunemann and

- 1
2
3 R. Kraehnert, *J. Am. Chem. Soc.* 2010, **132**, 1296–1301.
4
5
6 17 N. Toshima, T. Yonezawa and K. Kushihashi, *J. Chem. Soc., Faraday Trans.*, 1993, **89**,
7
8 2537–2543.
9
10 18 M.A. Faramarzi and H. Forootanfar, *Coll. Surf. B Biointerfaces*, 2011, **87**, 23–27.
11
12 19 Y. Nagata, Y. Mizukoshi, K. Okitsu and Y. Maeda, *Radiat. Res.* 1996, **146**, 333–338.
13
14 20 S. Ijima, *Nature*, 1991, **354**, 56–58.
15
16
17 21 T. Sehayek, M. Lahav, R. Popvitz-Biro, A. Vaskevich, and I. Rubinstein, *Chem. Mater.* 2005,
18
19 **17**, 3743–3748.
20
21 22 C.N.R. Rao and M. Nath, *J. Chem. Soc. Dalton Trans.*, 2003, **1**, 1–25.
22
23 23 D.T. Mitchell, S.B. Lee, L. Trofin, N. Li, T.K. Nevanen, H. Söderlund and C.R. Martin,
24
25 *J. Am. Chem. Soc.*, 2002, **124**, 11864–11865.
26
27
28 24 R.A. Caruso, J.H. Schattka and A. Greiner, *Adv. Mater.*, 2001, **13**, 1577–1579.
29
30 25 P. Blanchard, P. Leriche, P. Frere and J. Roncali, in *Advanced functional polythiophene based*
31
32 *on tailored precursors*, edn. T.A. Skotheim and J.R. Reynolds, CRC press, Florida, 2007. pp.
33
34 1–77.
35
36
37 26 L. Zhai and R.D. McCullough, *J. Mater. Chem.*, 2004, **14**, 141–143.
38
39 27 O. Surucu, G. Bolat and S. Abaci, *J. Electroanal. Chem.*, 2013, **701**, 20–24.
40
41
42 28 H. Aebi, *Methods Enzymol.*, 1984, **105**, 121–126.
43
44
45 29 W. Chen, W.P. Cai, C.H. Liang and L.D Zhang, *Mater. Res. Bull.*, 2001, **36**, 335–342.
46
47
48 30 T. Sakai, H. Enomoto, K. Torigoe, H. Sakai and M. Abe, *Coll. Surf. A Physicochemical. Eng.*
49
50 *Aspects*, 2009, **347**, 18–26.
51
52
53 31 K.S. Suslick, G.J. Price, *Annu. Rev. Mater. Sci.* 1999, **29**, 295–326.
54
55
56
57
58
59
60

- 1
2
3 32 S. Eliyahu, A. Vaskevich and I. Rubinstein, *Thin Solid Films*, 2010, **518**, 1661–1666.
4
5
6 33 K. Kwon, K. Y. Lee, Y. W. Lee, M. Kim, J. Heo, S. J. Ahn and S. W. Han, *J. Phys. Chem.*
7
8 *C*, 2006, **111**, 1161–1165.
9
10 34 K. C. Nguyen, *Adv. Nat. Sci.: Nanosci. Nanotechnol.*, 2012, **3**, 1–5.
11
12 35 A.J. Bard and L.R. Faulkner, *Electrochemical methods: fundamentals and applications*,
13
14 2nd edn. Wiley: New York, 2001.
15
16 36 N.Q. Jia, Z.Y. Wang, G.F. Yang, H.B. Shen and L.Z. Zhu, *Electrochem. Commun.*, 2007,
17
18 **9**, 233–238.
19
20
21 37 L. Wang, J. Wang and F. Zhou, *Electroanal.*, 2004, **16**, 627–632.
22
23 38 S.W. Ting, A.P. Periasamy, S.M. Chen and R. Saraswathi, *Int. J. Electrochem. Sci.*, 2011,
24
25 **6**, 4438–4453.
26
27
28 39 A.W. Bott and W.R. Heineman, *Current Separations*, 2004, **20**, 121–126.
29
30 40 S. Hashemnia, S. Khayatzadeh, A.A. Moosavi-Movahedi and H. Ghourchian, *Int. J.*
31
32 *Electrochem. Sci.* 2011, **6**, 581–595.
33
34
35 41 R.A. Kamin and G.S. Wilson, *Anal. Chem.*, 1980, **52**, 1198–1205.
36
37
38 42 M. Senel, E. Cevik and M.F. Abasiyanik, *Anal. Bioanal. Electrochem.*, 2011, **3**, 14–25.
39
40 43 P. Nien, T. Tung and K. Ho, *Electroanal.*, 2006, **18**, 1408–1415.
41
42
43 44 P. Arun Prakash, U. Yogeswaran and S.M. Chen, *Talanta*, 2009, **78**, 1414–1421.
44
45 45 Z. Liu, B. Zhao, Y. Shi, C. Guo, H. Yang and Z. Li, *Talanta*, 2010, **81**, 1650–1654.
46
47
48 46 Q. Sheng, M. Wang and J. Zheng, *Sensors and Actuators B*, 2011, **160**, 1070–1077.
49
50
51 47 A. Liu, W. Dong, E. Liu, W. Tang, J. Zhu and J. Han, *J. Electrochim. Acta*, 2010, **55**,
52
53 1971–1977.
54
55
56
57
58
59
60

Figure Captions

Fig. 1 Different electropolymerization parameters affecting the properties of the bioelectrode (A) Effect of concentration of thiophene (B) Effect of number of CV cycles (C) Effect of scan rate of polymerization on the electrode and (D) Electropolymerization of thiophene on bare Gr electrode at optimized parameters.

Fig. 2 (A) UV-Vis absorption spectra originating from SPR of AuNPs prepared by ultrasound irradiation. (B) The X-ray diffraction pattern of as-prepared AuNPs. (C) SEM images showing the spherical AuNPs obtained following sonochemical irradiation. (D) Typical particle diameter histogram.

Fig. 3 SEM of (A) surface of 200 nm pore diameter alumina membrane comprising of coalesced AuNPs before membrane dissolution, Inset is the SEM image of Gr/PTh/AuNPNTs after template dissolution and (B) Gr/PTh/AuNPNTs/EDC-NHS/CAT_{pp} modified electrodes. EDX patterns of (C) alumina template encompassing AuNPs, (D) Gr/PTh/AuNPNTs electrode and (E) Gr/PTh/AuNPNTs/EDC-NHS/CAT_{pp} modified electrodes. Insets are the quantitative results obtained from the EDX spectra of the corresponding electrodes.

Fig. 4 (A) CVs obtained at the bare Gr (a), Gr/PTh (b), Gr/PTh/AuNPNTs (c) and Gr/PTh/AuNPNTs/EDC-NHS/CAT_{pp} (d) modified electrodes in 5 mM Fe(CN)₆^{3-/4-} solution. (B) Niquist relationships of EIS data for bare Gr (a), Gr/PTh (b), Gr/PTh/AuNPNTs (c) and Gr/PTh/AuNPNTs/EDC-NHS/CAT_{pp} (d) modified electrodes. Inset displays the equivalent circuit used in the fit procedure of impedance spectra.

Fig. 5 (A) CVs of 5 mM H₂O₂ at (a)Gr/EDC-NHS/CAT_{pp}, (b) Gr/PTh/EDC-NHS/CAT_{pp}, (c) Gr/PTh/AuNPNTs and (d) Gr/PTh/AuNPNTs/EDC-NHS/CAT_{pp} electrode in 0.1 M PBS with

1
2
3 the scan rate of 50 mV s⁻¹. (B) Chronocoulometric responses of the Gr/PTh/AuNPNTs/EDC-
4 NHS/CAT_{pp} electrode in (a) absence and (b) presence of 2 mM H₂O₂ in 0.1 M nitrogen saturated
5
6
7
8
9 PBS solution.

10 **Fig. 6** (A) CV responses of Gr/PTh/AuNPNTs/EDC-NHS/CAT_{pp} electrode for different
11 concentrations (0, 1, 2, 4, 5,6,7 and 8 mM) of H₂O₂ in 0.1 M nitrogen saturated PBS solution.
12 Inset is the plot of peak current against added H₂O₂ concentration. (B) DPV curves obtained
13 upon step wise addition of increasing concentrations of H₂O₂ in neutral 0.1 M PBS for the
14 proposed Gr/PTh/AuNPNTs/EDC-NHS/CAT_{pp} electrode. Inset is the concentration dependence
15 of the peak currents obtained from the DPV measurements. (C) CVs of 2 mM H₂O₂ at the
16 Gr/PTh/AuNPNTs/EDC-NHS/CAT_{pp} electrode at different scan rates (a-l: 25, 50, 75, 100, 125,
17 150, 175, 200, 225, 250, 275 and 300 mV s⁻¹). Inset is the dependence of the anodic and cathodic
18 peak current on the square root of scan rate.
19
20
21
22
23
24
25
26
27
28
29
30
31

32 **Fig. 7** (A) Effect of operating potential  and temperature  on the CV response of the
33 modified electrode to 2 mM H₂O₂. (B) Dependence of anodic and cathodic peak currents of
34 2 mM H₂O₂ on pH values (3 to 10) of the solution at Gr/PTh/AuNPNTs/EDC-NHS/CAT_{pp}
35 electrode.
36
37
38
39
40

41 **Fig. 8** (A) Typical amperometric current response of the Gr/PTh/AuNPNTs/EDC-NHS/CAT_{pp}
42 electrode upon successive addition of various concentration of H₂O₂ at an applied potential of
43 -350 mV (vs. SCE) in 0.1 M PBS solution. Inset is the calibration plot of current versus H₂O₂
44 concentration. (B) The amperometric response of the modified bioelectrode to successive
45 additions of 2 mM H₂O₂ and interferences 200 μM DA (b), 1 mM AA (c) and 0.5 mM UA (d) in
46
47
48
49
50
51
52
53
54
55
56
57
58
59
60

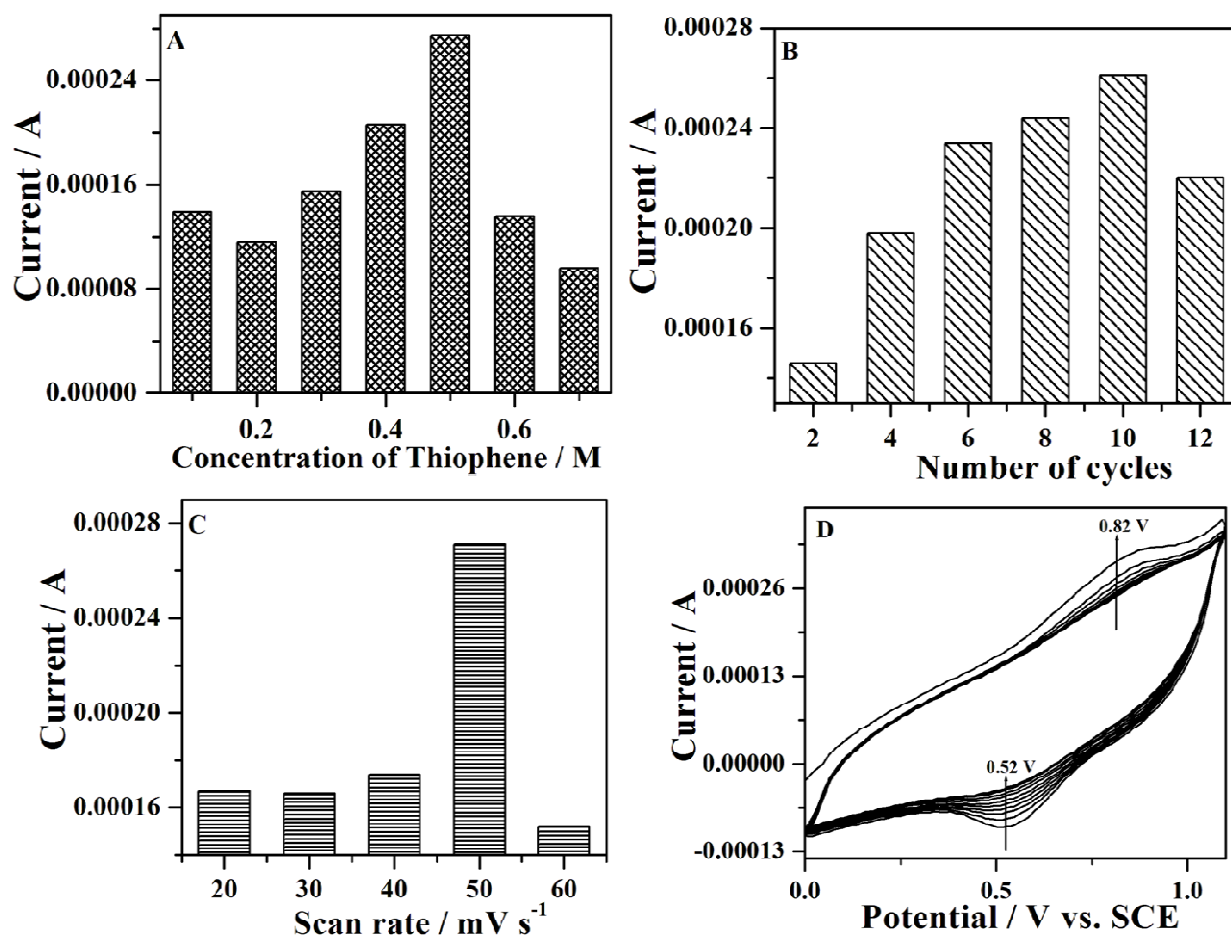


Fig. 1

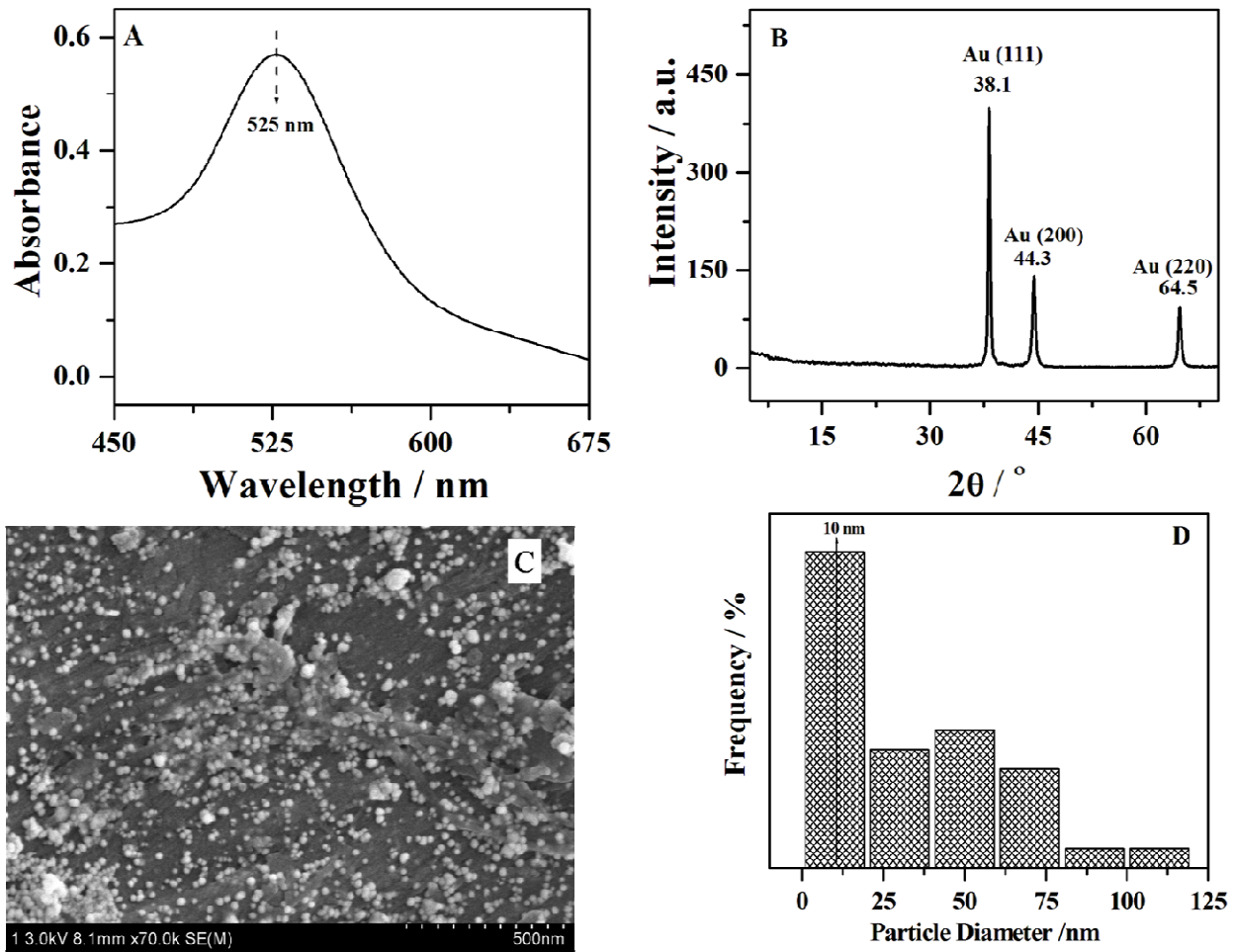


Fig. 2

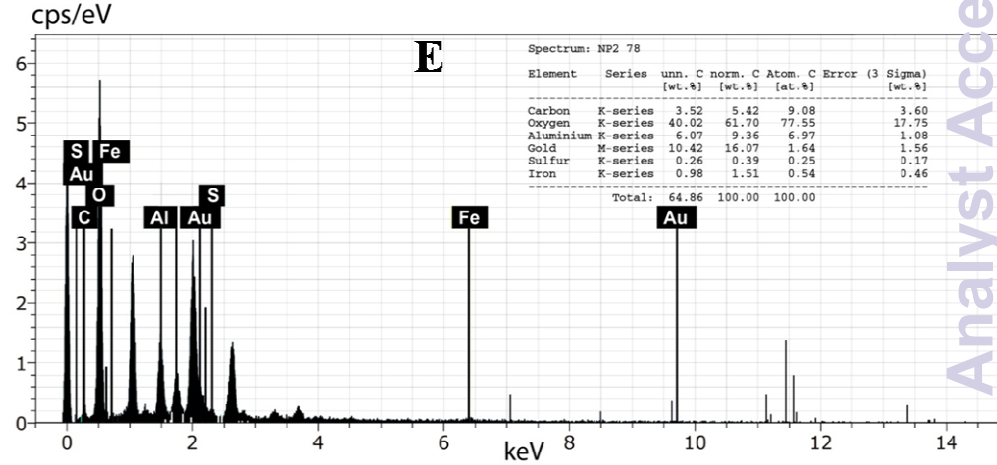
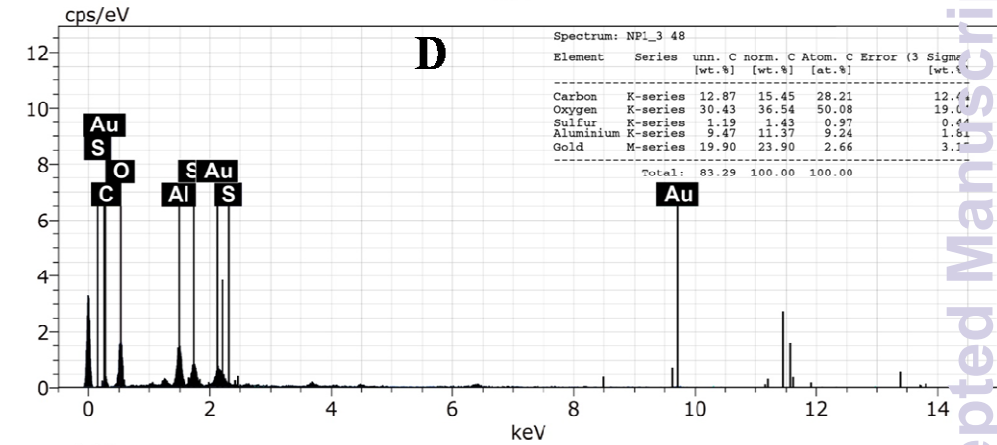
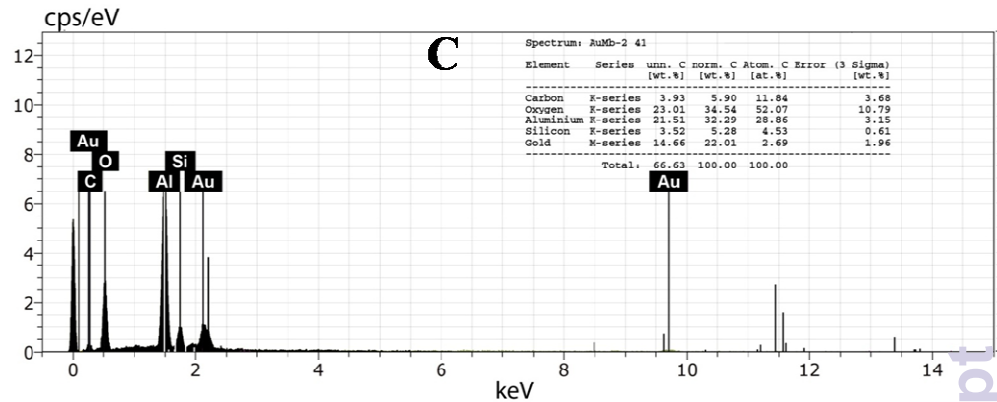
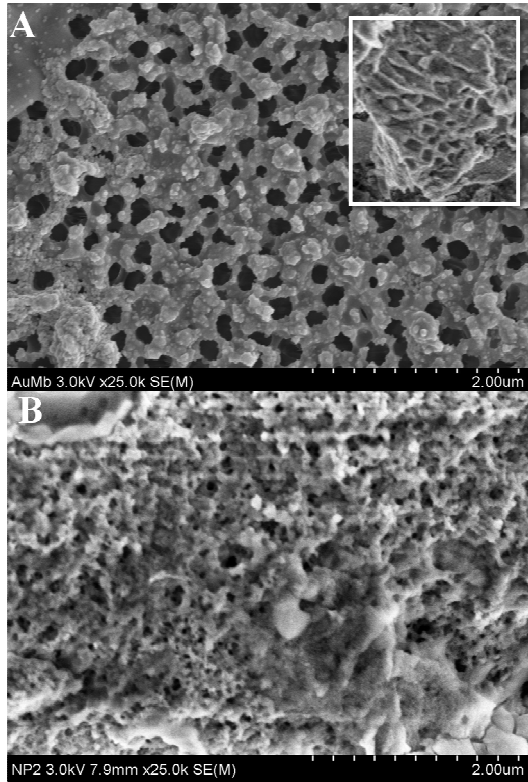


Fig. 3

Analyst Accepted Manuscript

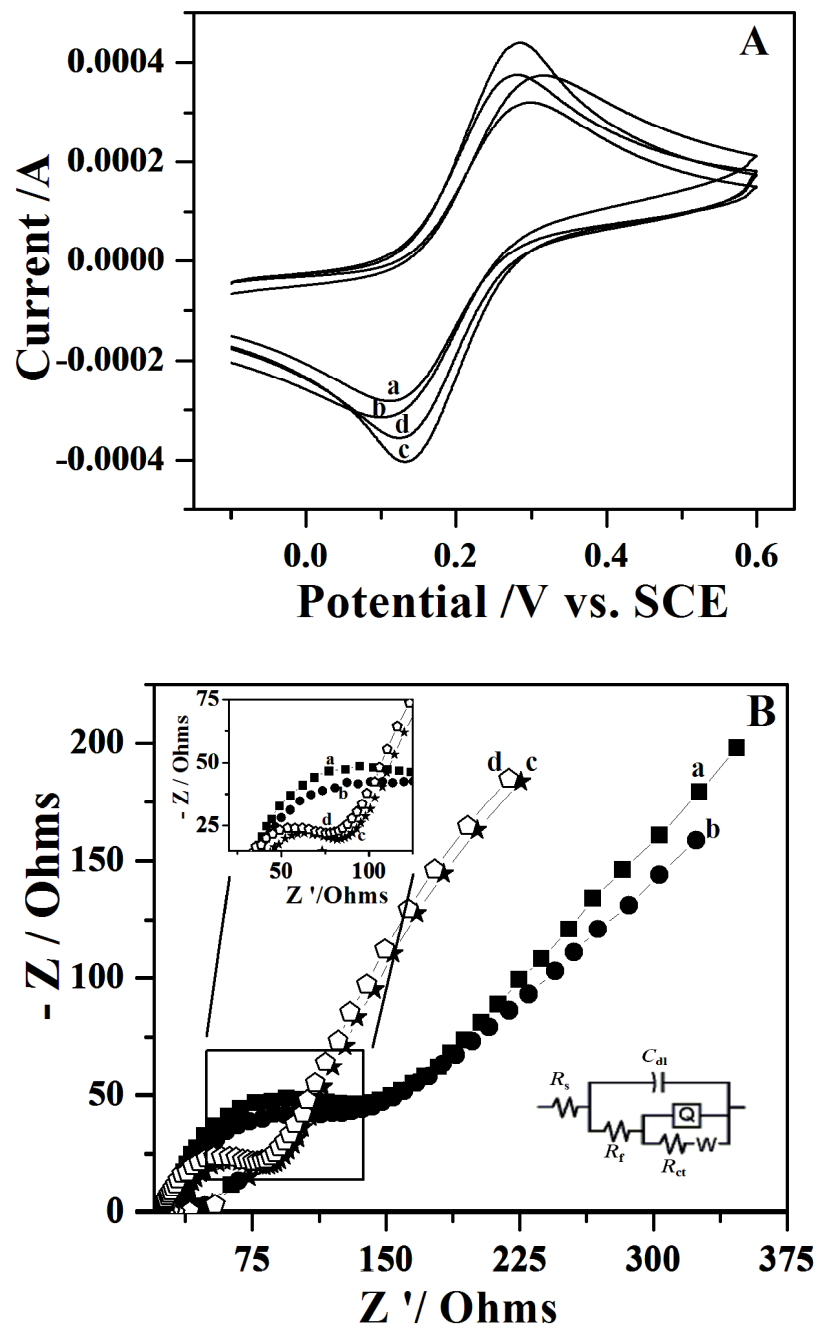


Fig. 4

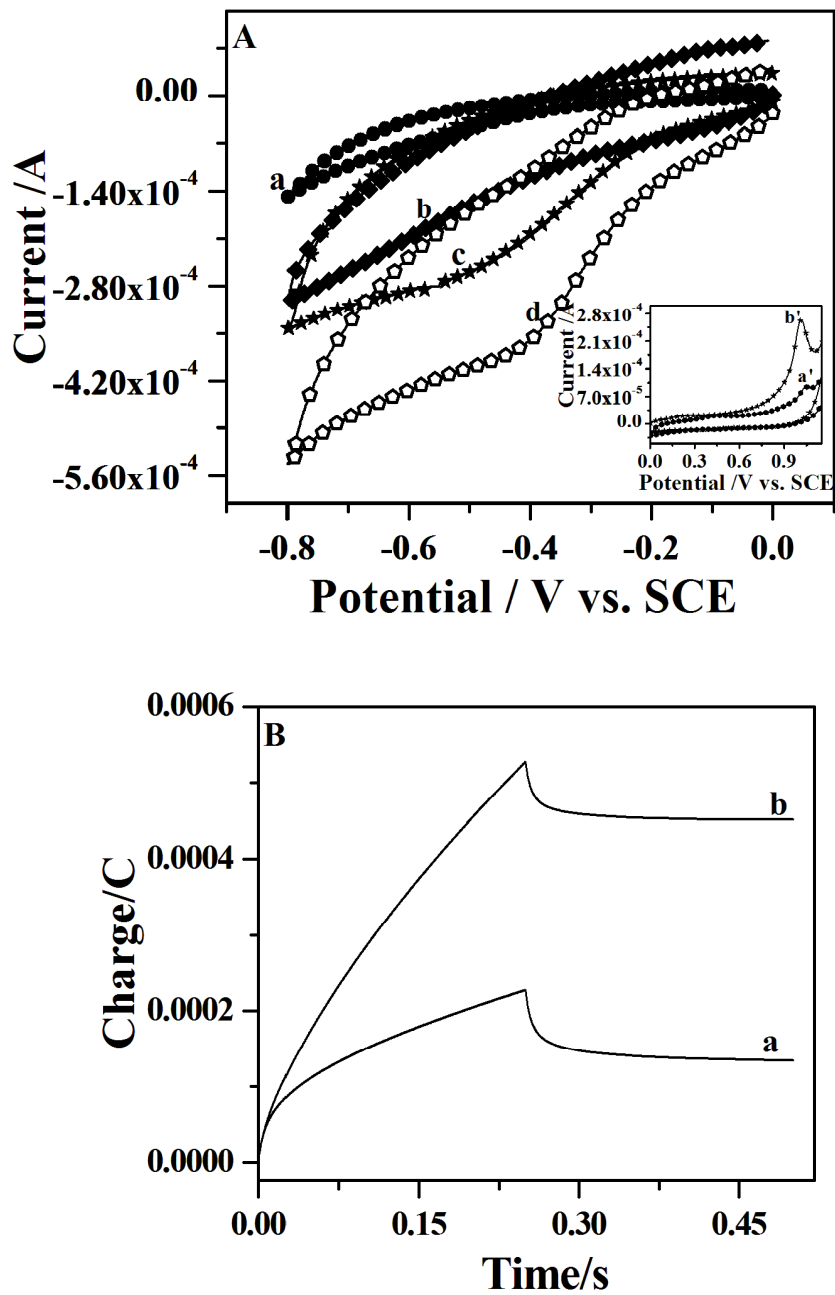


Fig. 5

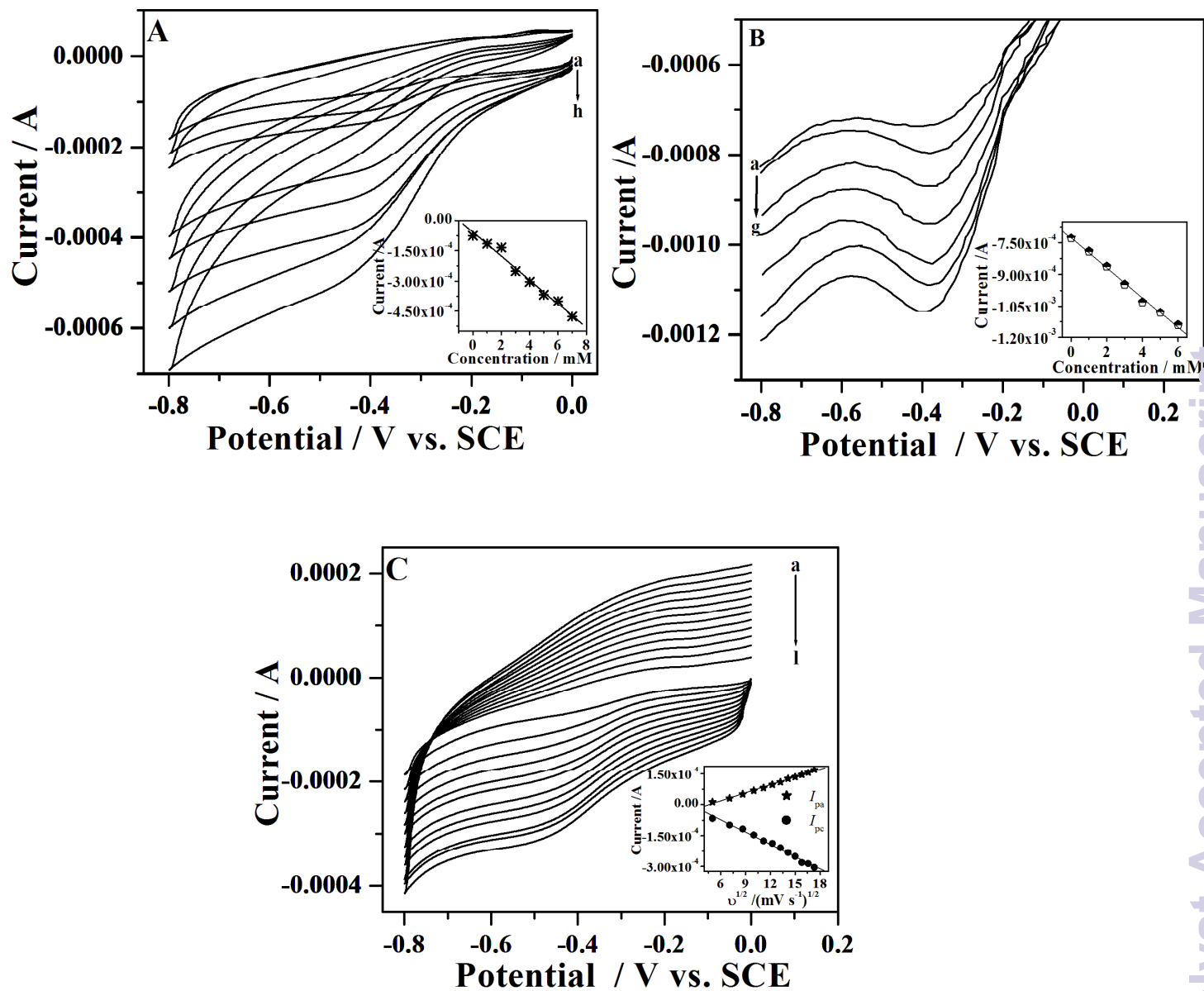


Fig. 6

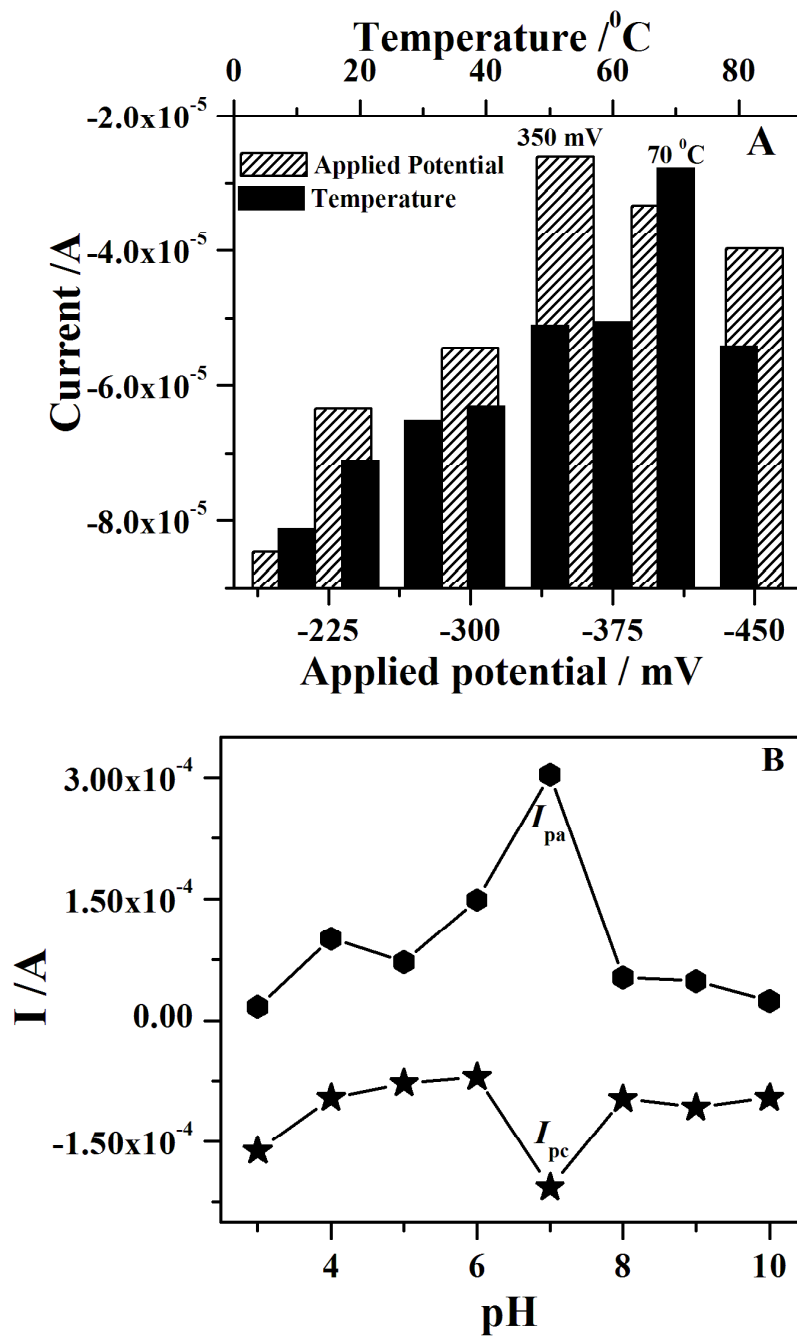


Fig. 7

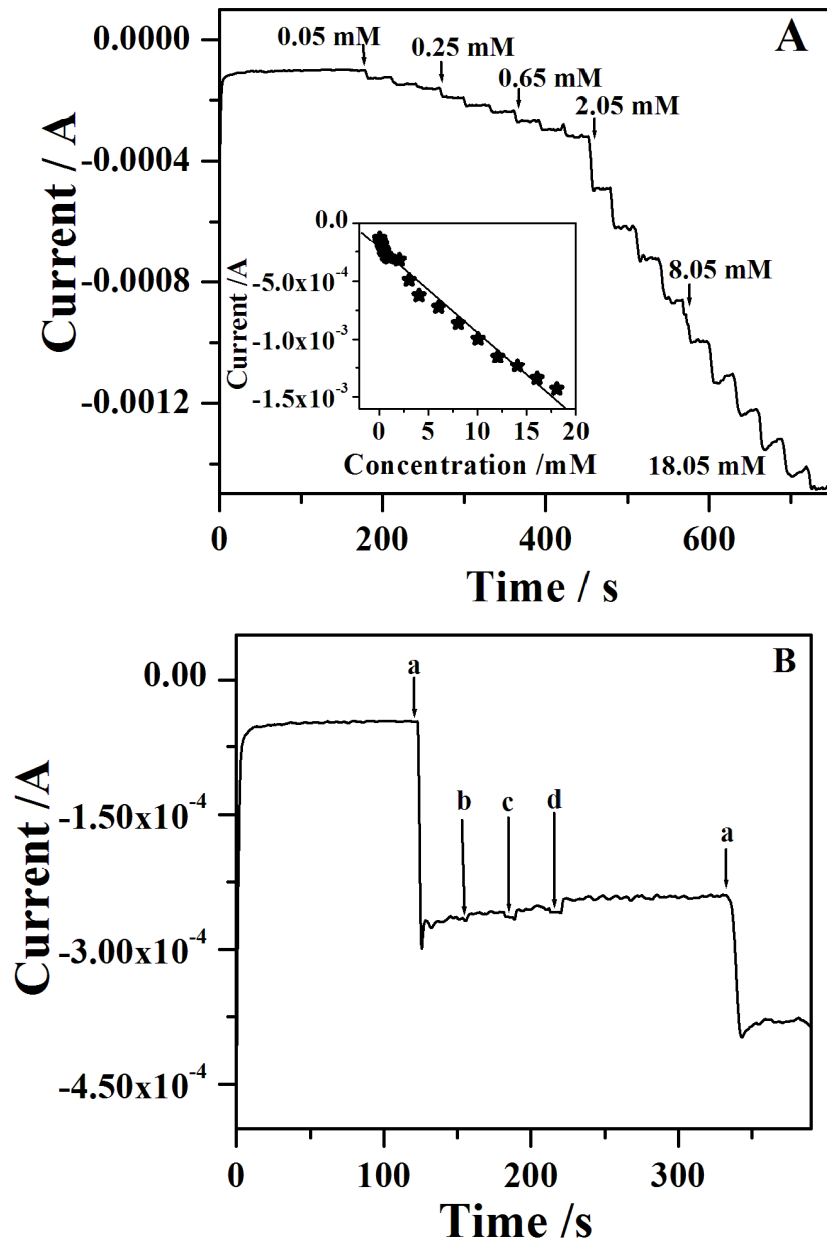


Fig. 8

Table 1. Impedance components for the Gr/PTh/AuNPNTs/EDC-NHS/CAT_{pp} electrodes determined by fitting EIS experimental data using the equivalent circuit

Electrode	R_s/Ω	C_{dl}/F	n	R_{ct}/Ω	R_f/Ω	W/Ω
bare Gr	34.84	2.95×10^{-5}	0.5	65.92	134.7	0.0018
Gr/PTh	36.68	2.58×10^{-5}	0.8	52.34	4.07×10^8	1.66×10^{-14}
Gr/PTh/AuNPNTs	39.98	5.47×10^{-5}	0.8	41.38	4.765	1.079
Gr/PTh/AuNPNTs/ EDC-NHS/CAT _{pp}	28.92	5.21×10^{-5}	0.6	44.73	218.3	0.0004

Table 2. Comparison of the beneficial analytical data obtained by the proposed with other electrochemical H₂O₂ sensor

H ₂ O ₂ electrochemical Sensor	Response Time/s	Linear range /mM	Detection limit / μ M	Sensitivity /mA mM ⁻¹ cm ⁻²	Ref
MWCNTs-Nf-(DDAB /CAT)	5	0.36 to 5.42	0.9	0.101	38
CAT/Poly(GMA-co-VFC)	<6	0.5 to 14	80	0.000034	42
Nf/CAT/ERGO	5	0.05 to 1.91	-	0.0077	43
Iron oxide- silver hybrid Modified GC electrode	3	0.0012 to 3.5	1.2	-	44
Ta-C:P/Au ₂ electrode	8	0.0002 to 1	0.08	0.00029	45
HRP/GE-CNT-Nafion /AuPt NPs/GCE	-	0.0005 to 0.1	0.17	0.370	46
Gr/PTh/AuNPNTs /EDC-NHS/ CAT _{pp}	7	0.05 to 18.5	0.12	26.2	This work